Reversible photobleaching of bacteriorhodopsin molecules exposed to 570 nm laser light

Gopalkrishna M. Hegde and K. P. J. Reddy*,#

Electronics and Computer Engineering Division, School of Engineering, Ngee Ann Polytechnic, Singapore 599 489
*Department of Aerospace Engineering, Indian Institute of Science, Bangalore 560 012, India

The phenomenon of reversible photobleaching in bacteriorhodopsin (BR) molecules exposed to 570 nm laser is presented. Creation of non-absorbing molecules in the bleached state is analysed theoretically using a simple theoretical model based on the excited-state absorption process. The analysis helps in ascertaining the percentage of molecules in the bleached state in the BR-based memory devices at any given time. The theory provides a bleaching parameter quantifying the number of photons the BR molecules can absorb before they reach a bleached state.

THE biological molecule bacteriorhodopsin (BR), which is found in the purple membrane of *Halobacterium halobium*, is finding many applications in the field of photonics due to its unique advantages[1–3]. The advantages of the BR molecule include high quantum efficiency of converting light into a state change, large absorption cross-section and nonlinearities, robustness to degeneration by environmental perturbations, capability to form thin films in polymers and gels, and existence of genetic variants with enhanced spectral properties for specific device applications[4–7]. The photochromic property of the BR molecule has resulted in applications like pattern recognition systems[8], three-dimensional memories[5], holography[9], second-harmonic generation[10], mode locking[11], spatial light modulation[12] and logic gates[3].

It is commonly known that one of the distinct differences between the widely used photochromic dyes and the BR molecules is the photobleaching effect, which severely limits the application of dyes in many optical devices[13]. In this communication we show that the BR molecule also suffers an equivalent bleaching mechanism due to the existence of the branched-photocycle. However, photobleaching in the BR molecule is reversible. Our main aim is to present the mechanism of reversible photobleaching in BR molecules in solid polymer matrix and to determine the bleaching parameter, defined as the average number of photons that the BR molecule absorbs before reaching the bleached state. The bleaching phenomenon described here is different from the photobleaching of purple membrane due to hydroxylamine presented recently, which occurs due to the disassembly of the purple membrane crystal into smaller crystals[14].

#For correspondence. (e-mail: laser@aero.iisc.ernet.in)

When exposed to light at 570 nm, the BR molecule undergoes a complex photocycle that generates intermediates shown in Figure 1. These intermediate states starting from the short-lived *J* state through *Q* state have absorption maxima spanning the entire visible region of the spectrum. The molecule can be switched to the original BR state, designated as *B* state, from any of the intermediate states using appropriate laser signal of peak wavelength indicated as indices in the photocycle. Except from the *P* and *Q* states, the BR molecule from all other intermediate states relaxes back into the original *B* state by thermal decay, as shown in the photocycle. However, the molecule in the *O* state can follow a branching path by absorbing appropriate photons and reach the *P* state instead of decaying to the *B* state. The molecule in the *P* state ultimately decays into the *Q* state, and hence we designate these states as a single *P*(*Q*) state. The molecule in the *Q* state has an absorption peak at 380 nm and has negligible absorption at 570 nm and hence remains in this state indefinitely, until exposed to 380 nm light. Thus the molecules which reach the *P*(*Q*) state are not available for the photochromic activity of the BR molecules excited by the 570 nm laser signal. This is equivalent to dye molecules reaching a bleached state which has negligible absorption at the excitation wavelength[15,16]. Hence, we define photobleaching of the BR molecule as the mechanism of exciting the BR molecule to the *P* state, which eventually decays into the *Q* state. Unlike the dye molecules, regeneration of the photobleached BR molecule into the original *B* state can be achieved by exposing the sample to 380 nm laser signal. Thus, photobleaching of the BR molecule exposed to 570 nm wavelength is completely reversible. Detailed analysis of the BR photocycle has been reported previously in a series of papers[12,17,18].

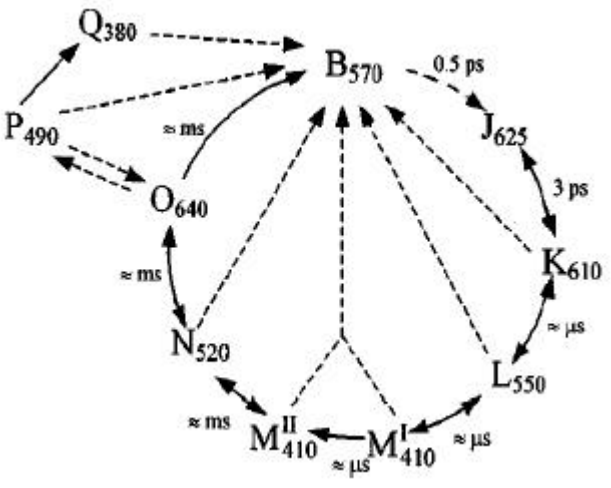

Figure 1. Schematic representation of the photochemical cycle indicating various intermediate states the BR molecule undergoes when exposed to 570 nm laser light. In the analysis, only *O* and *P*(*Q*) intermediate states are considered.

Transition from the *O* state to the *P* state is induced by exposing the BR sample simultaneously to 570 and 640 nm laser signals. The 570 nm signal transforms the BR to the *O* state, which has peak absorption at 640 nm to undergo a transformation to the *P* state, which eventually decays into the permanent *Q* state. This is the basic mechanism used in the development of BR-based logic gates and three-dimensional optical memories[3,5,7]. However, examination of the absorption spectra of the BR molecule and its intermediate states (see Figure 2, ref. 7) reveals that although the *O* state has an absorption peak at 640 nm, it has substantial absorption even at 570 nm. As a consequence, even in the absence of an excitation source at 640 nm, the BR molecule has a certain probability of undergoing the transition into the *P*(*Q*) state by absorbing a photon at 570 nm. Therefore, if the sample is exposed sufficiently long enough to the pump signal at 570 nm, it may attain a saturation state where the transmission reaches a maximum value. This is detrimental to the BR-based cache memories using $B \leftrightarrow M$ transition or permanent memories using $B \leftrightarrow K$ transition (working at cryogenic temperatures)[1,5]. In order to understand this phenomenon, we present a theoretical model of photoexcitation of the BR molecules to the *P*(*Q*) state when illuminated with a continuous laser light at 570 nm. This model involves an excited-state absorption process in which the BR molecules in the excited *O* state are progressively transformed into a permanent bleached state, which has negligible absorption at 570 nm. The analytical solutions presented here help in ascertaining the percentage of total BR molecules in the photobleached state at any given time. The analysis yields a photobleaching parameter B_l for each BR molecule, defined as the average number of photons that it can absorb before reaching the bleached state.

The theoretical model presented here is based on the model proposed for the dye molecules[15,16]. We assume uniform distribution of the BR molecules in solid polymer matrix with volumetric concentration of N_0 and the population in the *P*(*Q*) state created progressively during the illumination of the sample. When exposure starts at time $t = 0$, all the BR molecules are present in the ground state represented as the *B* state. We assume a simplified photocycle for the BR molecule where only the intermediate *O* state is considered, and we assume that the molecule once excited to the *P* state will eventually reach the *Q* state (thus the *P* and *Q* states are treated as degenerate states). Since the bleaching phenomenon is dependent only on the population density of the *O* intermediate state, neglecting the other intermediate states of the BR photocycle will have no effect on the bleaching parameter presented in this analysis. We assume CW light at 570 nm to be incident in the *z*-direction with $z = 0$ at the input face of the sample of thickness *L*. Let $N_B(z, t)$, $N_O(z, t)$ and $N_P(z, t)$ be the population densities of the BR species in the *B*, *O* and *P*(*Q*) states, respectively, such

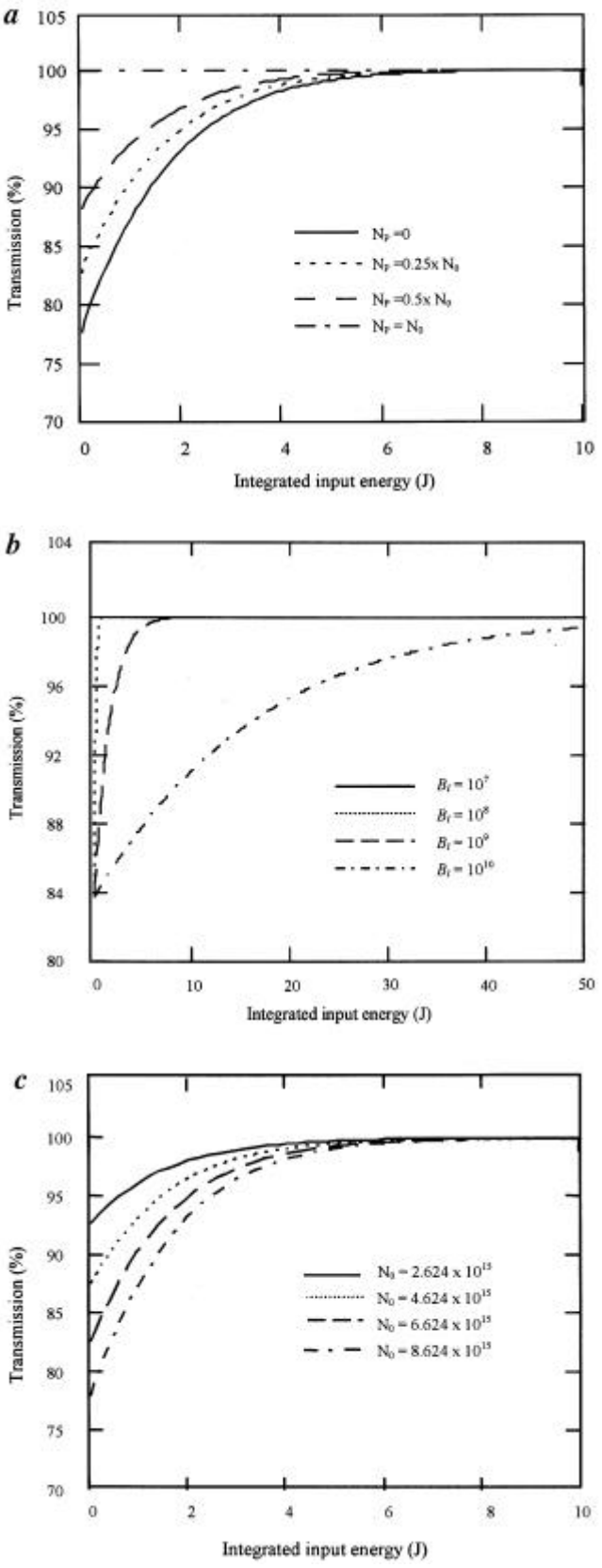

Figure 2. Variation of percentage of transmission of BR sample with the integrated input energy for (***a***) different population densities in the *P*(*Q*) state, (***b***) different values of the bleaching parameter, and (***c***) different doping concentrations.

that $N_B(z,t)+N_O(z,t)+N_P(z,t)=N_0$. The equation for the total population can also be written in terms of the number of molecules per unit area in length z as:

$$J_B(z,t)+J_O(z,t)+J_P(z,t)=N_0 z,$$

where, $J_B(z,t)=\int_0^z N_B(z',t)\mathrm{d}z'$,

$$J_O(z,t)=\int_0^z N_O(z',t)\mathrm{d}z' \text{ and } J_P(z,t)=\int_0^z N_P(z',t)\mathrm{d}z'.$$

For the sample length of L, we can write $J_B(L,t)+J_O(L,t)+J_P(L,t)=N_0L=J_0$.

The local flux of photons at 570 nm can be written as:

$$n(z,t)=n_0\exp[-\sigma_B\gamma_{BK}J_B(L,t)-\sigma_O\gamma_{OP}J_O(L,t)], \quad (1)$$

where n_0 is the incident flux of photons, σ_B and σ_O are the absorption cross-sections of the BR molecule in the B and O states respectively, and γ_{BK} and γ_{OP} are the quantum efficiencies of $B\to K$ and $O\to P$ transitions respectively. In eq. (1) we have neglected the contribution by the BR population in the $P(Q)$ state, as the absorption at 570 nm is at least two orders of magnitude less than that of the BR molecules in either the B or the O state. We can rewrite eq. (1) in terms of the number of BR molecules per unit area as:

$$n(z,t)=n_0\exp[-\Delta\sigma J_B(z,t)]\exp[-\sigma_O\gamma_{OP}(N_0z-J_P(z,t))], \quad (2)$$

where $\Delta\sigma=(\sigma_B\gamma_{BK}-\sigma_O\gamma_{OP})$.

We can write the local rate of transition to the $P(Q)$ state, i.e. bleaching rate as:

$$\frac{\partial N_B(z,t)}{\partial t}=-\sigma_B\gamma_{BK}N_B(z,t)B_l^{-1}n(z,t)+\frac{N_O(z,t)}{\tau}. \quad (3)$$

Here, the first term is the absorption at 570 nm by the molecules in the B state and the second term is due to the thermal decay of the molecules in the O state to the B state with relaxation time of τ. The parameter B_l is the average number of photons absorbed by a BR molecule before reaching the $P(Q)$ state. Integrating both sides over thickness L and using eq. (2) we get the total bleaching rate:

$$\frac{\mathrm{d}J_B(L,t)}{\mathrm{d}t}=-\sigma_B\gamma_{BK}B_l^{-1}n_0\int_0^L N_B(z,t)\exp[-\Delta\sigma J_B(z,t)]\times\exp[-\sigma_O\gamma_{OP}(N_0z-J_P(z,t))]\mathrm{d}z+\int_0^L\frac{N_O(z,t)}{\tau}\mathrm{d}z. \quad (4)$$

Equation (4) can be rewritten in terms of the number of BR molecules per unit area in length as:

$$\frac{\mathrm{d}J_B(L,t)}{\mathrm{d}t}=-\frac{\sigma_B\gamma_{BK}B_l^{-1}n_0}{\Delta\sigma}\int_0^L\frac{\partial}{\partial z}[-\Delta\sigma J_B(z,t)]\exp[-\Delta\sigma J_B(z,t)]\times\exp[-\sigma_O\gamma_{OP}(N_0z-J_P(z,t))]\mathrm{d}z+\int_0^L\frac{1}{\tau}\frac{\partial}{\partial z}J_O(z,t)\mathrm{d}z. \quad (5)$$

Equation (5) can be solved analytically with the approximations $\exp[-\sigma_O\gamma_{OP}(N_0z-J_P(z,t))]=1$ and $J_O(L,t)=0$. The first approximation is possible if $\sigma_O\gamma_{OP}(N_0z-J_P(z,t))\ll 1$, when $0\le z\le L$. Therefore, the condition for the validity of the approximation is $\sigma_O\gamma_{OP}N_0L\ll 1+\sigma_O\gamma_{OP}J_P(L,t)$. The second approximation implies that the integrated population in the O state is zero at any given time. This approximation is true because the O state is truly a transient state from which the molecule will either decay into the B state or get excited to the $P(Q)$ state with the absorption of an additional photon at 570 nm. With these approximations, eq. (5) reduces to:

$$\frac{\mathrm{d}J_B(L,t)}{\mathrm{d}t}=-\frac{\sigma_B\gamma_{BK}B_l^{-1}n_0}{\Delta\sigma}\{\exp[-\Delta\sigma J_B(z,t)]-1\}. \quad (6)$$

Integrating eq. (6) with the initial condition $J_B(L,0)=J_0$, we get:

$$\exp[-\Delta\sigma J_B(L,t)]=\frac{1}{1+\{\exp[\Delta\sigma(J_0-J_P(L,0))]-1\}\exp(-\sigma_B\gamma_{BK}B^{-1}n_0t)}. \quad (7)$$

From this equation we can write the evolution of the number of BR molecules per unit area in terms of the integrated input energy per unit area, $E=n_0h\nu t$, where h is the Planck's constant and ν is the frequency of laser light, as:

$$\frac{J_B(L,E)}{J_B(L,0)}=\frac{\ln[1+\{\exp[\Delta\sigma(J_0-J_P(L,0))]-1\}\exp(-\beta E)]}{\Delta\sigma(J_0-J_P(L,0))}, \quad (8)$$

where $\beta=(\sigma_B\gamma_{BK}/h\nu)B_l^{-1}$.

The transmission through the BR sample given by $T(t)=n(L,t)/n_0$ can be written with the help of eq. (2) as:

$$T(t) = \exp[-\Delta\sigma J_B(L, t)] \exp[-\sigma_O \gamma_{OP}(J_0 - J_P(L, 0))]. \quad (9)$$

Using eq. (7), eq. (9) yields the transmission in terms of the integrated input energy as:

$$T(E) = \frac{\exp[-\sigma_O \gamma_{OP}(J_0 - J_P(L, 0))]}{1 + \{\exp[\Delta\sigma(J_0 - J_P(L, 0))] - 1\}\exp(-bE)}. \quad (10)$$

Finally, defining the small-signal transmission as $T(0) = \exp[-\sigma_B \gamma_{BK}(J_0 - J_P(L, 0))]$ and the saturated signal transmission as $T(\infty) = \exp[-\sigma_O \gamma_{OP}(J_0 - J_P(L, 0))]$, we can rewrite eq. (10) as:

$$T(E) = \frac{T(\infty)}{1 + [T(\infty)/T(0) - 1]\exp(-bE)}. \quad (11)$$

The analytical solutions presented here are useful to study the influence of different system parameters on the temporal evolution of transmission for the BR sample with the integrated input energy of the laser light in the presence of photobleaching of the BR molecules. The transmission characteristics are computed for a BR sample thickness of 0.25 cm, with the absorption cross-sections $\sigma_B = 2.4 \times 10^{-16}$ cm^2 and $\sigma_O = 1.1 \times 10^{-16}$ cm^2, and the quantum efficiencies $\gamma_{BK} = 0.64$ and $\gamma_{OP} = 2 \times 10^{-4}$ at 570 nm (ref. 18). The total doping concentration of BR is selected such that the condition $\sigma_O \gamma_{OP}(N_0 L - J_P(L,t)) \ll 1$, used for obtaining the analytical solutions, is satisfied. However, by comparing the analytical solutions with the complete numerical solutions, it was shown that the analytical solutions given here can be used even for higher doping concentrations limited by $\sigma_O \gamma_{OP}(N_0 L - J_P(L,t)) < 0.5$. For the results presented here, the doping concentration of BR is selected such that the latter condition is satisfied.

The temporal evolution of percentage of transmission of the BR sample as a function of the integrated input energy of the pump beam at 570 nm with a BR concentration of 1.1×10^{-4} mol/l and bleaching parameter $B_l = 10^9$ is shown in Figure 2 *a* for different values of the percentage of BR molecules in the permanent $P(Q)$ state. It is seen that in the absence of molecules in the $P(Q)$ state, the percentage of transmission increases gradually from a minimum to a maximum value, which is typical of the transmission behaviour of pure BR molecules at 570 nm (ref. 18). For the case of all BR molecules excited to the $P(Q)$ state, it is seen that the transmission is 100%. Since the absorption cross-section of the BR molecules in the $P(Q)$ state at 570 nm is negligible, the probe beam passes through the sample without being attenuated. Thus, by examining the transmission characteristics of the BR sample at 570 nm, the present theory helps to predict the percentage of molecules in the nonparticipating $P(Q)$ state. This is an important issue in the case of BR-based cache memories using *B* and *M* states, as well as the three-dimensional memories using *B* and *K* states at cryogenic temperatures[1,5]. If the transmission characteristics reach towards that of the fully occupied $P(Q)$ state, it is essential to reset the sample by exposing it to the 380 nm light beam. Otherwise the efficiency of the BR-based memories will be drastically affected.

The analytical expressions are further used to investigate the effect of bleaching parameter B_l and the BR concentration on the transmission characteristics with fixed percentage of molecules in the $P(Q)$ state. The variation of percentage of transmission as a function of the integrated input laser energy is shown in Figure 2 *b* and *c* for various cases. It is seen that the bleaching parameter does not affect the small signal or saturated transmission of the BR sample, but just affects the rate of photoexcitation of the molecules to the $P(Q)$ state. It is observed that the bleaching factor reported here is about an order of magnitude higher than the corresponding factor for the dye molecules in solid matrix[15,16]. However, the exact value of the bleaching factor can be obtained only by matching the theoretically predicted curves with the experimental results. From Figure 2 *c* it is seen that the BR concentration affects the small-signal transmission and the rate of photobleaching, while it has no effect on the saturated-signal transmission.

In conclusion, we have discussed the phenomenon of reversible photobleaching in the BR molecules in contrast to the permanent photobleaching in dye molecules. Unlike the dye molecules, the photobleached BR molecules can be reset by exposing them to light at 380 nm. The theoretical analysis of the photobleaching phenomenon presented here using the simple theoretical model based on the excited-state absorption of the BR molecules in the *O* state, helps in monitoring the percentage of molecules reaching the bleached $P(Q)$ state by repeated exposure to 570 nm probe beam. An important application of this analysis is that it helps in monitoring the efficiency of the BR-based memories operated using 570 nm laser beam.

1. Osterhelt, D., Brauchle, C. and Hampp, N., Bacteriorhodopsin: a biological material for information processing. *Q. Rev. Biophys*., 1991, **24**, 425–428.
2. Hampp, N., Bacteriorhodopsin as a photochromic retinal protein for optical memories. *Chem. Rev*., 2000, **100**, 1755–1776.
3. Sukhdev Roy, Singh, C. P. and Reddy, K. P. J., Analysis of all-optical switching in bacteriorhodopsin. *Curr. Sci.*, 2002, **83**, 623–627.
4. Birge, R. R., Photophysics and molecular electronics applications of the rhodopsins. *Annu. Rev. Phys. Chem.*, 1990, **41**, 683–733.
5. Birge, R. R., Protein-based computers. *Sci. Am*., 1995, **272**, 90–95.
6. He, J. A., Samuelson, L., Li, L., Kumar, J. and Tripathy, S. K., Bacteriorhodopsin thin film assemblies–immobilization, properties and applications. *Adv. Mater*., 1999, **11**, 435–446.

7. Birge, R. R. *et al*. Protein based associative processors and volumetric memories. *J. Phys. Chem. B*, 1999, **103**, 10746–10766.
8. Hampp, N., Thoma, R., Zeisel, D. and Brauchle, C., Bacteriorhodopsin variants for holographic pattern recognition in molecular and biomolecular electronics. *Adv. Chem*., 1994, **240**, 511–526.
9. Downie, J. D. and Smithey, D. T., Measurement of holographic properties of bacteriorhodopsin films. *Appl. Opt*., 1996, **35**, 5780–5789.
10. Huang, J. Y., Chen, Z. and Lewis, A., Second-harmonic generation in purple membrane-poly(vinyl alcohol) films: probing the dipolar characteristics of the bacteriorhodopsin chromophore in bR570 and M412. *J. Phys. Chem.*, 1989, **93**, 3314–3320.
11. Reddy, K. P. J., Passive mode locking of lasers using bacteriorhodopsin molecules. *Appl. Phys. Lett.*, 1994, **64**, 2776–2778.
12. Reddy, K. P. J., Analysis of light-induced processes in bacteriorhodopsin and its application for spatial light modulation. *J. Appl. Phys*., 1995, **77**, 6108–6113.
13. Ippen, E. P., Shank, C. V. and Dienes, A., Rapid photobleaching of organic laser dyes in continuously operated devices. *IEEE J. Quantum Electron*., 1971, **QE-7**, 178–179.
14. Moller, C., Buldt, G., Dencher, N. A., Engel, A. and Muller, D. J., Reversible loss of crystallinity on photobleaching purple membrane in the presence of hydroxylamine. *J. Mol. Biol*., 2000, **301**, 869–879.
15. Dubois, A., Canva, M., Brun, A., Chauput, F. and Boilot, J. P., Photostability of dye molecules trapped in solid matrices. *Appl. Opt*., 1996, **35**, 3193–3199.
16. Dubois, A., Canva, M., Brun, A., Chauput, F. and Boilot, J. P., Enhanced photostability of dye molecules trapped in solid xerogel matrices. *Synth. Metals*, 1996, **81**, 305–308.
17. Sukhdev Roy and Reddy, K. P. J., Modelling of light modulation processes in D85N bacteriorhodopsin. *Curr. Sci.*, 2000, **78**, 184–188.
18. Sukhdev Roy, Singh, C. P. and Reddy, K. P. J., Generalized model of all-optical light modulation in bacteriorhodopsin. *J. Appl. Phys*., 2001, **90**, 3679–3688.

ACKNOWLEDGEMENT. This work was performed while K.P.J.R. was at Nee Ann Polytechnic as a consultant.

Received 3 June 2003; revised accepted 10 October 2003

Synoptic hydrology of India from the data of isotopes in precipitation

S. K. Gupta* and R. D. Deshpande

Physical Research Laboratory, Navrangpura, Ahmedabad 380 009, India

Recently, regional maps of amount weighted monthly isotopic data of precipitation have become available from the GNIP/IAEA database (http://isohis.iaea.org). These maps are based on stations for which at least one complete year of isotopic and precipitation data were available. In this communication an attempt has been made to discern and describe the hydrological processes responsible for giving characteristic regional distribution of $\delta^{18}O$ and '*d*-excess' for different seasons over the Indian subcontinent. It is shown that the characteristic isotopic signal is imparted to precipitation initially by the two primary oceanic sources of vapour influx, namely the Arabian Sea and the Bay of Bengal during both the summer and winter monsoon seasons. Subsequently, the processes of evaporation and transpiration redistribute and recycle the water between the atmosphere and the land surface. The isotopic data help in identifying the geographical regions where any source/process dominantly influences the precipitation signal.

PRECIPITATION is of major interest in the hydrologic cycle as it is the primary source of water on land. Therefore, an understanding of the formation of precipitation and its variations are important to a hydrologist. Similarly, understanding the processes controlling temporal and geographic variations of isotopic composition of precipitation is equally important to an isotope hydrologist. The meteoric processes modify the isotopic composition of water in such a way that precipitation in a particular environment has a characteristic isotopic signature. This signature then serves as a natural tracer for the provenance of groundwater. Characterizing the stable isotope distribution in meteoric waters is, therefore, essential in determining the input function for most isotopic hydrology applications.

Realizing the importance of the basic data on isotopic composition of precipitation to hydrology, the International Atomic Energy Agency (IAEA), in collaboration with World Meteorological Organization (WMO) established the Global Network of Isotopes in Precipitation (GNIP) at which samples are collected to monitor the $\delta^{18}O$ and δD of precipitation. The data produced by this network are available on the World Wide Web at http://isohis.iaea.org.

In the Indian context, the Arabian Sea (AS)[1] and the Bay of Bengal (BOB) are the two oceanic moisture sources that primarily feed the rainfall during two seasons, namely southwest summer monsoon (June–September) and northeast winter monsoon (October–January, refs 2 and 3; C. K. Rajan, unpublished). In addition, locally recycled vapour from within and around India as also long-distance transport of vapour under the influence of western disturbances contribute to rainfall[2]. These vapour sources are expected to have characteristic isotopic signatures. Further, evaporation from falling raindrops under the conditions of low humidity and high temperature in parts of the country during certain periods can impart distinctive isotopic signatures to rainfall. The isotopic composition of precipitation can therefore be used to discern the influence of different vapour sources and post-precipitation processes. In the following, starting with some relevant basic concepts, an attempt is made to describe the hydrological processes responsible for giving characteristic regional distribution of $\delta^{18}O$ and '*d*-excess' for different seasons over the Indian subcontinent.

*For correspondence. (e-mail: skgupta@prl.ernet.in)